Calorimetric low temperature detectors for low-energetic heavy ions and their application in accelerator mass spectrometry

S. Kraft-Bermuth,[1,a)] V. A. Andrianov,[1,b)] A. Bleile,[1] A. Echler,[1] P. Egelhof,[1] A. Kiseleva,[1] O. Kiselev,[1,c)] H. J. Meier,[1] J. P. Meier,[1] A. Shrivastava,[1,d)] M. Weber,[1] R. Golser,[2] W. Kutschera,[2] A. Priller,[2] P. Steier,[2] and C. Vockenhuber[2]
[1]*Gesellschaft für Schwerionenforschung GSI, D-64291 Darmstadt, Germany and Institut für Physik, Johannes Gutenberg Universität, D-55099 Mainz, Germany*
[2]*Vienna Environmental Research Accelerator, Institut für Isotopenforschung und Kernphysik, Universität Wien, A-1090 Wien, Austria*

(Received 13 May 2009; accepted 9 August 2009; published online xx xx xxxx)

The energy-sensitive detection of heavy ions with calorimetric low temperature detectors was investigated in the energy range of $E=0.1-1$ MeV/amu, common for accelerator mass spectrometry (AMS). The detectors used consist of sapphire absorbers and superconducting aluminum transition edge thermometers operated at $T\sim 1.5$ K. They were irradiated with various ion beams (^{13}C, ^{197}Au, ^{238}U) provided by the VERA tandem accelerator in Vienna, Austria. The relative energy resolution obtained was $\Delta E/E=(5-9)\times 10^{-3}$, even for the heaviest ions such as ^{238}U. In addition, no evidence for a pulse height defect was observed. This performance allowed for the first time to apply a calorimetric low temperature detector in an AMS experiment. The aim was to precisely determine the isotope ratio of $^{236}U/^{238}U$ for several samples of natural uranium, ^{236}U being known as a sensitive monitor for neutron fluxes. Replacing a conventionally used detection system at VERA by the calorimetric detector enabled to substantially reduce background from neighboring isotopes and to increase the detection efficiency. Due to the high sensitivity achieved, a value of $^{236}U/^{238}U=6.1\times 10^{-12}$ could be obtained, representing the smallest $^{236}U/^{238}U$ ratio measured at the time. In addition, we contributed to establishing an improved material standard of $^{236}U/^{238}U$, which can be used as a reference for future AMS measurements. © *2009 American Institute of Physics.* [doi:10.1063/1.3213622]

I. INTRODUCTION

Accelerator mass spectrometry (AMS) is a well established method for the determination of very small isotope ratios with high sensitivity.[1] In comparison with conventional mass spectrometry, the use of accelerated ion beams provides substantial advantages in the quality of isotope separation and background suppression, thus allowing the determination of isotope ratios down to a level of $10^{-10}-10^{-16}$, depending on the ion species. ^{236}U represents one of the heaviest nuclides of interest for AMS. Being produced in nature by capture of thermal neutrons in the reaction $^{235}U(n,\gamma)^{236}U$ and having a half-life of 23.4×10^6 yr,[2] the relative abundance of ^{236}U provides an excellent neutron flux monitor integrated over geological time scales. Thus, besides other applications, ^{236}U could be used to prove the existence of an enhanced neutron flux due to natural "reactorlike" conditions in the past.[3] In natural uranium minerals, the isotope ratio is expected to be of the order of $10^{-10}-10^{-14}$, dependent on the sample's history and surroundings. However, the energy resolution and detection efficiency of conventional heavy ion detection systems limit the sensitivity and demand relatively large amounts of sample material.[4]

Conventional heavy ion detectors, such as semiconductor detectors, which operate on a charge collection principle, are limited in energy resolution, especially at very low kinetic energies, by considerable losses in the ionization signal of up to 60%–80%, which appear due to direct phonon excitation by nuclear scattering processes as well as due to charge recombination (the latter effect is dominant for very heavy ions due to extremely high charge densities) and result in a substantial pulse height defect. Furthermore, the detection efficiency of such detectors is limited by ion losses in entrance windows or dead layers and especially for very heavy ions semiconductor detectors suffer from considerable radiation damage even after short periods of irradiation.

Calorimetric low temperature detectors use an alternative detection concept: a calorimetric detector measures the temperature rise of an absorber after the energy deposited by the incident particle has been converted into heat. This detection principle is schematically displayed in Fig. 1: the incident particle deposits its kinetic energy E by electronic and nuclear stopping processes (for details see Ref. 5) in an absorber with a heat capacity C at an operating temperature T_a. After thermalization of the whole absorber, a temperature

[a)]Author to whom correspondence should be addressed. Electronic mail: kraftber@uni-mainz.de.
[b)]Present address: Institute of Nuclear Physics, Lomonosov Moscow State University, Vorob'evy Gory, Moscow 119992, Russia.
[c)]Present address: Paul Scherrer Institut, 5232 Villigen PSI, Switzerland.
[d)]Present address: Nuclear Physics Division, Bhabha Atomic Research Center, Trombay, Mumbay 400085, India.

 © 2009 American Institute of Physics

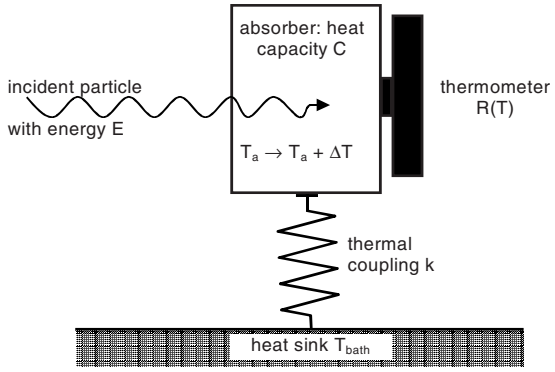

FIG. 1. Schematic principle of particle detection with a calorimetric low temperature detector (discussion see text).

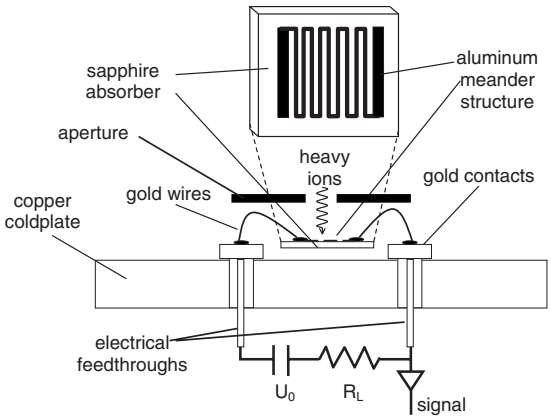

FIG. 2. The setup of a calorimetric detector with a superconducting aluminum TES is schematically displayed.

rise $\Delta T = E/C$ is induced. To realize a large temperature change, low heat capacities and thus low operating temperatures are essential. The temperature rise ΔT is then read out by determining the resistance change of a temperature-dependent resistor $R(T)$. High dR/dT values for high resistance changes are realized either by specially doped semiconductors or by a superconductor operated at the transition temperature [transition edge sensor (TES)]. The dynamic behavior of the detector is determined by the heat capacity C as well as the thermal coupling constant k (see Refs. 6 and 7 for a detailed discussion). A detailed overview of such detectors and their applications can be found in Ref. 8.

The detection principle of calorimetric detectors can provide considerable advantages over conventional charge-collecting detectors for heavy ions in several regards.[9] As in principle almost the whole deposited energy is finally converted into heat after the decay of the initial electronic excitations, a more complete energy detection is achieved, which considerably reduces fluctuations in the detected amount of energy, and therefore improves the energy resolution. Furthermore, these detectors do not necessarily need entrance foils such as ionization chambers or dead layers such as semiconductor detectors. As a consequence, a considerable reduction of detection threshold and energy straggling is obtained, providing increased detection efficiency and energy resolution for low-energetic heavy ions. As the detection principle is to a large extent independent of material properties except the specific heat and the thermal conductivity, the absorber material can be optimized for heavy ion detection by choosing a material with high resistivity against radiation damage.

Calorimetric detectors for heavy ions have already been demonstrated[6,10–12] to provide an excellent relative energy resolution of $\Delta E/E = (1-2) \times 10^{-3}$ for energetic heavy ions in a wide range of ion species (^{20}Ne$\cdots^{238}$U) and energies ($E = 5-360$ MeV/amu). Therefore, they bear a large potential for various applications in heavy ion research. Especially when replacing conventional heavy ion detectors in AMS experiments, they can improve the sensitivity by their higher detection efficiency, lower detection threshold and better background suppression due to their excellent energy resolution. As AMS is commonly performed at dedicated tandem accelerators with a relatively small terminal voltage of 0.5–5 MeV, energies for heavier ions usually do not exceed 0.3 MeV/amu. Therefore, the first aim of the investigations discussed in this paper was to extend studies of the performance of calorimetric detectors to the energy range of $E = 0.1-1$ MeV/amu. The results allowed to apply such detectors for the first time in an AMS experiment to precisely determine the isotope ratio ^{236}U/^{238}U in several samples of natural uranium minerals.

II. DETECTOR DESIGN AND EXPERIMENTAL SETUP

Within the past 15 years, two types of calorimetric low temperature detectors for heavy ions with different thermistors, one on the basis of a semiconducting germanium thermistor,[10] the other one on the basis of a superconducting TES,[11,12] have been developed. Because the TES calorimeters provide higher sensitivities for low energies as compared to detectors with germanium calorimeters, the present investigations were performed using the TES calorimeters. These detectors consist of a thin superconducting aluminum film serving as the TES and operated at $T \sim 1.5$ K (see also Fig. 2). Using photolithographic techniques, a 10 nm thick aluminum film, which is evaporated onto a sapphire substrate with a thickness of 330 μm and an area of approximately 2×3 mm^2, serving as the absorber, is etched to a 10 μm wide strip with a total length of 52 mm in a meanderlike structure. At the transition temperature $T_C \sim 1.5$ K this leads to a resistance of typically $R_C \sim 15$ kΩ, sufficiently high for conventional preamplifiers to be used for signal readout. The width of the transition covers a range of 2 mK $\leq \delta T \leq$ 10 mK. Figure 3 displays a typical transition curve. A more detailed discussion of layout and preparation of the detectors can be found in Refs. 6, 7, and 11.

The experimental setup is shown schematically in Fig. 4. The detectors were mounted onto the cold finger of a pumped ^{4}He bath cryostat operated at temperatures between 1.2 and 1.6 K. The operating temperature was regulated using an electric control circuit; a temperature stabilization with fluctuations of the order of 1 μK was obtained. To avoid energy straggling and efficiency losses of the low-energetic heavy ions, entrance windows were replaced by four entrance slits of dimensions 2×30 mm^2 for the systematic investigations and of 3.5×15 mm^2 for the AMS measurements, respectively.

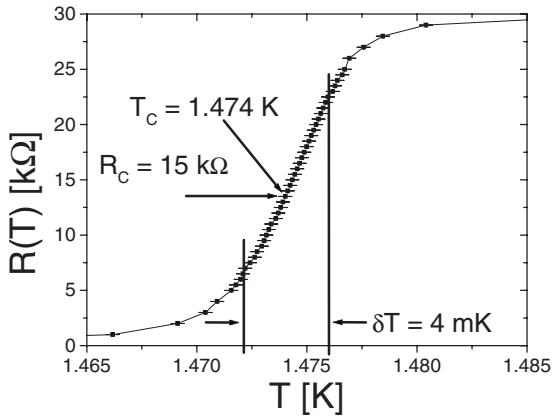

FIG. 3. A typical $R(T)$ characteristic: T_C is the transition temperature and δT represents the width of the transition.

The cryostat was connected to the beamline of the Vienna Environmental Research Accelerator (VERA) (Ref. 3) in Vienna, Austria. A cesium sputter ion source produces negative ions which are injected into a tandem accelerator with 3 MV terminal voltage. A high resolving magnetic and electrostatic analyzing system provides heavy ion beams of various ions in an energy range of 6 MeV$\leq E \leq$65 MeV with an energy spread as small as $\Delta E/E \leq 10^{-4}$.

For the systematic investigation of detector response, the 0°-beamline was used. The count rate was adjusted via a slit system to about 10–50 s^{-1}. For a direct comparison, a conventional silicon surface barrier detector was mounted at the same beamline and could be moved in front of the calorimetric detector, thus allowing measurements with both detectors under practically identical experimental conditions.

To suppress background from neighboring uranium isotopes, an additional switching magnet (see Sec. IV) had to be used for the AMS measurements. Therefore, these measurements were performed at the 20°-beamline. The count rate of the radioisotope ^{236}U was detected in the calorimetric detector, while for the long-lived ^{238}U the beam current was measured in a Faraday cup which was moved in and out of the beam.

To minimize systematic errors, several targets for the ion source had been prepared from each sample (for details of target preparation see Ref. 3); these targets were measured several times in cyclic order, one measurement lasting 600 s. In these measurements, count rates for ^{236}U ranged from 10 s^{-1} down to 10^{-2} s^{-1} for the sample with the lowest ^{236}U abundance. The measurements were performed by an automated measurement routine of VERA, described in detail in Ref. 13. The ^{236}U count rate was evaluated in the following way: As all components in the spectrum have very sharply defined energies (see Sec. IV), the spectrum was deconvoluted into Gaussian line shapes for the different isotopes. The amplitude of each Gaussian normalized to the measurement time gave the actual count rate for each component. The ^{238}U current was measured alternating every 200 s. To determine the transmission through the beamline, the count rate of ^{236}U in the calorimetric detector was compared to the count rate in a conventional silicon detector with approximately 100% detection efficiency which was positioned in front of the cryostat (see Fig. 4). For a detailed description of the AMS measurement procedure see also Refs. 3 and 4. In contrast to the setup described in these references, no time-of-flight (TOF) detector was included in the present measurements.

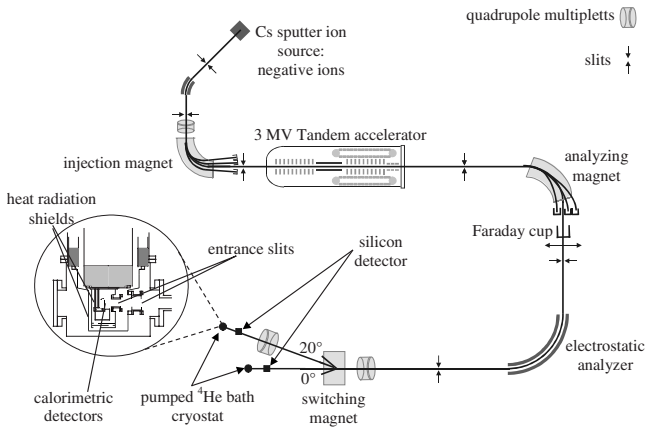

FIG. 4. Schematic view of the experimental setup: the pumped ^{4}He bath cryostat was connected directly to the beamline of the VERA. For the systematic investigations the 0°-beamline was used. The AMS measurements were performed at the 20°-beamline (for details see text).

III. SYSTEMATIC INVESTIGATION OF DETECTOR PERFORMANCE UNDER IRRADIATION WITH LOW-ENERGETIC HEAVY IONS

The response of calorimetric detectors to the impact of low-energetic heavy ions was studied using ^{13}C, ^{197}Au, and ^{238}U beams at various incident energies ranging from E=10 MeV to E=60 MeV, corresponding to 0.1$\leq E \leq$1 MeV/amu. In addition, data for 5.5 MeV α-particles provided by a ^{239}Pu/^{241}Am/^{244}Cm source mounted inside the cryostat were taken.

A preamplifier signal for the impact of a ^{238}U ion with E=17.39 MeV is displayed in Fig. 5(a). The relatively short thermal decay time of τ=206 μs allows for count rates up to about 0.5–1 kHz. The corresponding energy spectrum is displayed in Fig. 5(b). The solid line is the result of a fit with a Gaussian to the data resulting in a width of ΔE_{FWHM}=80 keV. This corresponds to a relative energy resolution of $\Delta E/E = 4.6 \times 10^{-3}$, which represents the best result obtained at energies below 1 MeV/amu at present. The shoulder on the low energy side is caused by ions scattered off the entrance slits.

As compared to conventional ionization detectors, this result represents a considerable improvement in energy resolution, especially at these relatively low ion energies. Figure 6 compares the spectrum of the calorimetric detector to that of the conventional silicon surface barrier detector for ^{238}U ions at E=20.85 MeV. Even though the performance of the calorimetric detector was somewhat worse due to different experimental conditions, the resolution of $\Delta E/E = 7.4 \times 10^{-3}$ is about one order of magnitude better than the resolution of $\Delta E/E = 57 \times 10^{-3}$ achieved with the silicon detector. Furthermore, a relatively fast decrease in the energy resolution of the silicon detector throughout several hours of measuring time was observed, most probably due to radiation damage.

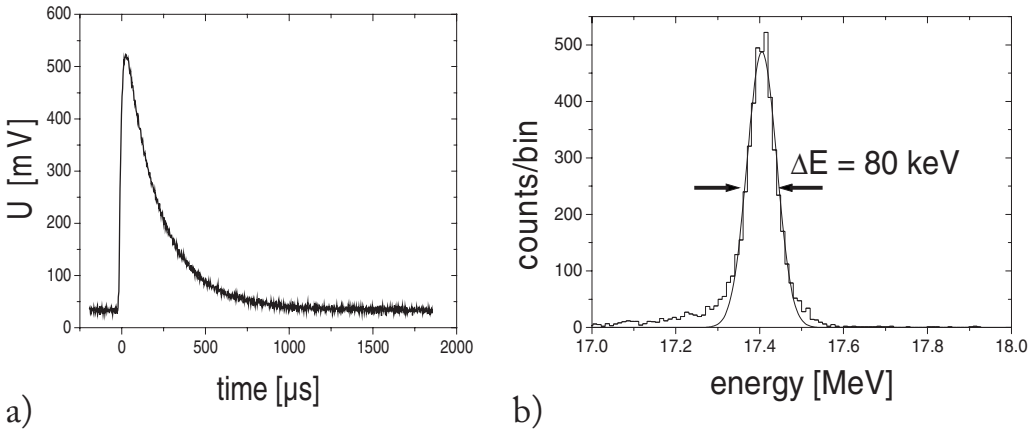

FIG. 5. (a) Preamplifier signal and (b) energy spectrum for ^{238}U ions at $E=17.39$ MeV obtained with the aluminum TES calorimeter. The relative energy resolution achieved was $\Delta E/E=4.6\times10^{-3}$ (Ref. 14).

In contrast, the calorimetric detector showed no evidence of such behavior even after irradiation with integrated ion doses of 10^9 ions/cm^2.

Results of a systematic study on the relative energy resolution, obtained for all ions and energies investigated, are summarized in Fig. 7; as the measurement for ^{238}U at $E=17.39$ MeV was performed during the AMS measurements in a different experimental setup, this measurement is not included. At low energies ($E<20$ MeV), an increase of $\Delta E/E$ for α-particles and ^{13}C is observed. This behavior may be explained by a lack of sensitivity of the present detectors due to their relatively large heat capacity, and could be improved in future by using substantially thinner absorbers as compared to $d=330$ μm in the present setup. For energies $E\geq20$ MeV, the relative energy resolution is approximately constant, independent of ion species and incident energy. The solid line is the result of a fit to the data using the following ansatz:

$$\frac{\Delta E}{E}=\frac{1}{E}\cdot\sqrt{\Delta E_{\mathrm{BLN}}^2+(\beta\cdot E)^2}.$$

Hereby, ΔE_{BLN} represents the contribution of the baseline noise which is supposed to limit the signal-to-noise-ratio for low energies and describes the increase in energy resolution for $E<20$ MeV. For higher energies, the term $\Delta E\sim E$ dominates, β being a proportional constant. This term is most probably due to intrinsic detector properties. It can, e.g., be caused by a position dependence of the detector response function due to incomplete thermalization of the whole absorber.[16] Further detailed investigation of the energy deposition processes will be necessary for a full understanding of the observed detector performance. The fit yields a result of $\beta=6.93(5)\times10^{-3}$. This result confirms that the improvement in energy resolution by one order of magnitude as compared to conventional ionization detectors was not only achieved for ^{238}U, but for all ions investigated.

Figure 8(a) summarizes the results of investigations on the linearity of detector response. A perfectly linear behavior as a function of energy is obtained over the entire range of ions from ^{4}He up to ^{238}U. The solid line represents a linear fit to the data. Even more remarkable, the peak positions for the three different ions ^{13}C, ^{197}Au, and ^{238}U at the same energy agree within 0.1%, showing no evidence of a pulse height defect. In contrast, for the conventional silicon detector a considerable pulse height defect of 70% was observed when comparing the peak position of ^{13}C to the one of ^{238}U [Fig. 8(b)].

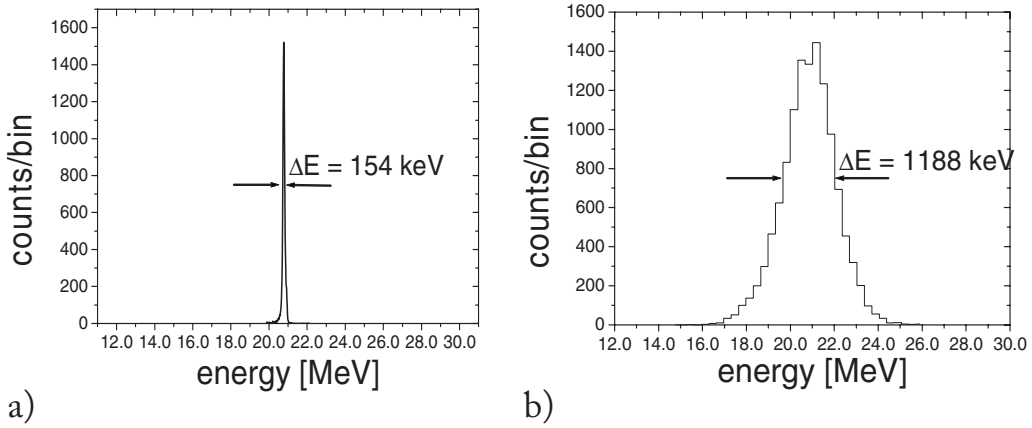

FIG. 6. Energy spectra for ^{238}U ions at $E=20.85$ MeV taken under identical experimental conditions with (a) the aluminum TES calorimeter and (b) the silicon surface barrier detector. The relative energy resolution achieved was $\Delta E/E=7.4\times10^{-3}$ for the calorimetric and $\Delta E/E=57\times10^{-3}$ for the silicon detector, respectively.

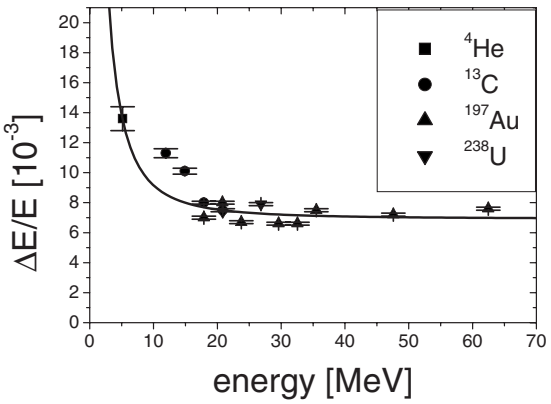

FIG. 7. Summary of a systematic study of the detector performance for various ions and energies. Relative energy resolution obtained for various ions (^{4}He, ^{13}C, ^{197}Au, ^{238}U) in an energy range of E=5–60 MeV. The solid line represents a fit to the data (for discussion see text) (Ref. 15).

These results allow to set an upper limit on the existence of Z-dependent energy loss processes. Such loss processes are due to the creation of local lattice defects, so-called *Frenkel pairs*, which give rise to phonon trapping, i.e., the creation of long-lived metastable electronic states with lifetimes much longer than the thermal time constant of the detector. The energy stored in such trapped phonons consequently does not contribute to the thermal signal. As the number of Frenkel pairs created is proportional to the nuclear stopping power,[17] the effect is expected to contribute more for very slow and very heavy ions, for which nuclear stopping dominates the energy transfer process. From the nonexistence of a pulse height defect as well as the fact that the energy resolution is independent of the ion species, it can be concluded that such Z-dependent energy loss processes are indeed negligible in calorimetric low temperature detectors.[18]

IV. APPLICATION IN AN AMS EXPERIMENT: PRECISE DETERMINATION OF THE ISOTOPE RATIO ^{236}U/^{238}U IN NATURAL URANIUM

The excellent energy resolution makes calorimetric low temperature detectors suitable instruments for AMS, especially for investigations with very heavy ions such as ^{236}U. Under the experimental conditions at the VERA AMS facility, background in AMS measurements for very heavy ions such as ^{236}U is mainly due to neighboring isotopes (^{234}U, ^{235}U, ^{238}U), which undergo charge exchange reactions with the residual gas in the accelerator beamline, and afterwards have the same magnetic rigidity ME/q^2 as ^{236}U (M being the mass and q the charge state of the ion). Therefore, the neighboring isotopes can pass through the high-energy magnetic analyzer and—after additional charge exchange— also through the electrostatic analyzer (see Ref. 3 for a detailed discussion). The background situation expected for the case of ^{236}U^{5+} at E=17.54 MeV is displayed in Fig. 9. As the resolution of the magnetic analyzer is very high (see Ref. 3), the condition ME/q^2=constant leads to well defined energies for the background peaks.

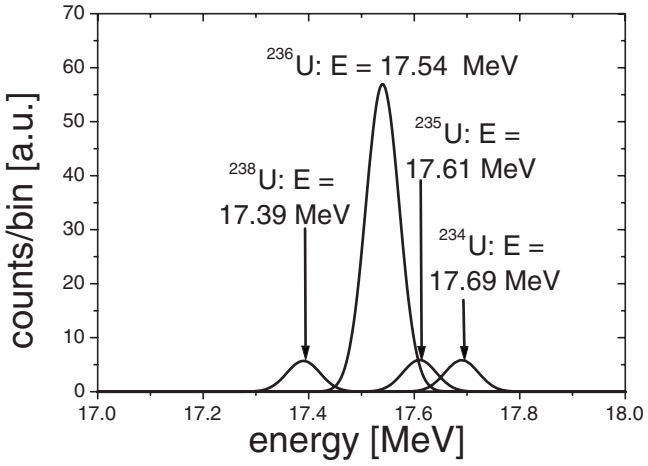

FIG. 9. Simulation of background situation under the assumption of Gaussian line shapes. The ratio of ^{236}U to ^{238,235,234}U is assumed to be 10:1, the energy resolution to be $\Delta E/E$=4.6×10^{-3} (Ref. 14).

Since standard heavy ion detectors (e.g., ionization chambers) do not provide sufficient energy resolution to resolve these background peaks, in the standard measurement procedure[3,4] a TOF spectrometer combined with an ionization chamber is used. Due to ion losses in the foils of the

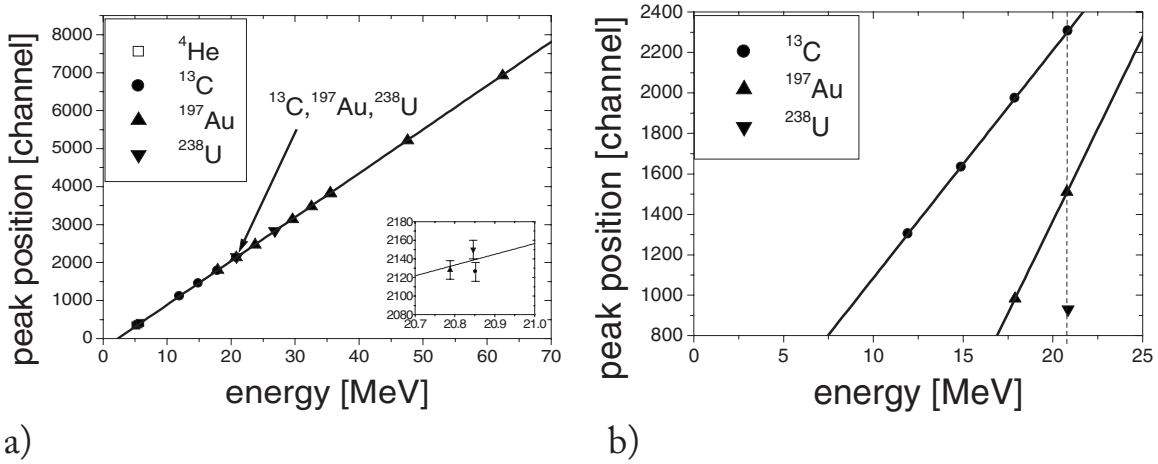

FIG. 8. Summary of a systematic study of the detector performance for various ions and energies. Linearity of energy response obtained for various ions (^{4}He, ^{13}C, ^{197}Au, ^{238}U) in an energy range of E=5–60 MeV for (a) the calorimetric detector and (b) for a conventional silicon surface detector. The solid lines represent fits to the data. The inlay shows the point at E=20.8 MeV in an enlarged scale (Ref. 15).

TABLE I. Results of the measurements $^{236}U/^{238}U$ isotope ratio to establish a material standard (Vienna-KkU and Joachimsthal 2) and to improve the sensitivity (Bad Gastein). The systematic error results from the determination of the transmission.

Sample	$^{236}U/^{238}U[10^{-11}]$
Vienna-KkU	$3.89 \pm 0.08_{stat} \pm 0.35_{syst}$
Joachimsthal *2*	$2.29 \pm 0.07_{stat} \pm 0.29_{syst}$
Vienna-KkU[a]	$6.98 \pm 0.32_{stat} \pm 0.68_{syst}$
Bad Gastein	$0.61 \pm 0.17_{stat} \pm 0.12_{syst}$

[a]Reference 20.

TOF detector and the entrance window of the ionization chamber, transmission through this detection system is limited to 31%,[19] thus limiting the sensitivity.[4] With a relative energy resolution of $\Delta E/E = 4.6 \times 10^{-3}$ as achieved for calorimetric detectors, it is possible to distinguish the isotope of interest from the neighboring isotopes by the high energy-resolving power of the detector alone (see Fig. 9). Thus, replacing the conventional TOF/ionization-chamber detection system by a calorimetric detector leads to a substantially improved sensitivity, especially important for the detection of very rare isotopes.

The present experiment has two aims.

- *Establishing a material standard*. To minimize systematic errors caused by changes in machine performance and experimental setup, AMS measurements are usually performed normalized to a material standard for which the isotope ratio is very precisely known. In the case of $^{236}U/^{238}U$, such a material standard had not been established due to lack of a suitable material (see also Ref. 4). However, the VERA laboratory possesses a considerable amount of uranyl nitrate from the mine *Joachimsthal*, prepared and stored before 1918 and thus not contaminated by ^{236}U created by human nuclear activities. This material, in the following referred to as *Vienna-KkU*, is therefore very suitable as a material standard. Steier *et al.*[4,20] performed first measurements on this material with a conventional energy/TOF detection system; their result is displayed in Table I together with the results of the measurements presented here. The first aim of the experiment with the calorimetric detector was to determine the isotope ratio $^{236}U/^{238}U$ in two samples from the mine Joachimsthal to improve the precision of the material standard value.
- *Increasing the sensitivity*. One sample investigated had been extracted from 5 l of water stemming from a uranium containing spring in the region of *Bad Gastein*, Austria. As the uranium in the water had been washed out from the deep regions of the Alps, the isotope ratio was not known, but expected to be significantly lower than that of the uranyl nitrate.

V. RESULTS OF THE AMS EXPERIMENT

For the very first AMS measurement performed with a calorimetric detector, the detector performance under running conditions was unfortunately worse as compared to the results presented in Sec. III, mainly due to an increase in the heat capacity of the detector by condensation of residual gas onto the detector surface. However, already with a resolution of $\Delta E/E = 9.1 \times 10^{-3}$, essential parts of background could be separated; whereas a possible contribution of ^{235}U is still included in the ^{236}U count rate. Results of the measurements are summarized in Table I, including statistical and systematic errors. The systematic error is mainly limited by the determination of the transmission from the Faraday cup to the detector. As compared to a conventional detection system, using a calorimetric detector improved the transmission from $(31 \pm 3)\%$ to $(65 \pm 10)\%$, in the latter case limited by the active detector area.

A. Samples from Joachimsthal

The spectrum for the sample Vienna-KkU is displayed in Fig. 10(a). As compared to the total count rate, background contribution from ^{234}U is 10(1)% and from ^{238}U 4(1)%. Therefore, at a level of 10^{-11}, background is no limitation of sensitivity. As compared to the conventional setup, statistical as well as systematic errors have been improved considerably. The result of the Vienna-KkU sample in our measurements agrees reasonably well with the result of Steier *et al.*, but it is clearly smaller. The reason for this discrepancy is yet unclear and has to be investigated in detail in a future measurement campaign. The result of the sample Joachimsthal 2, the energy spectrum of which is displayed in Fig. 10(b), is

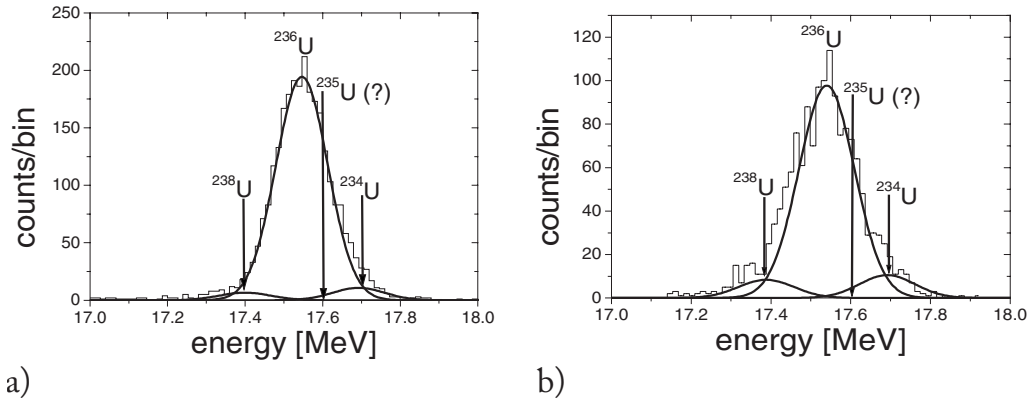

FIG. 10. Energy spectrum for the AMS measurement of the $^{236}U/^{238}U$ isotope ratio in the samples (a) Vienna-KkU and (b) Joachimsthal 2.

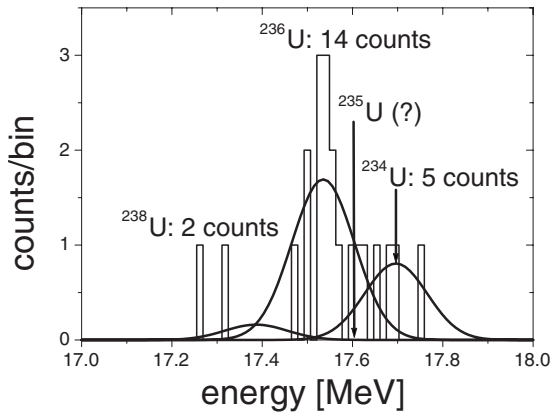

FIG. 11. Energy spectrum for the AMS measurement of the $^{236}U/^{238}U$ isotope ratio in the sample prepared from Bad Gastein spring water.

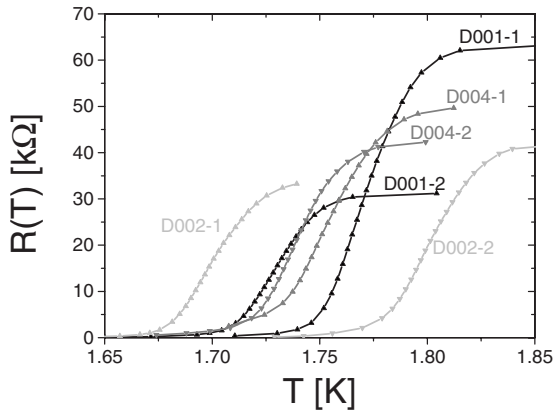

FIG. 12. Examples for several different transition curves for different detectors are shown. All detectors were produced on one single sapphire wafer in one production run.

again considerably smaller than the result of Vienna-KkU. However, this is understandable because the sample originates from a different batch of Joachimsthal ore and local variations of rock composition, e.g., presence or absence of neutron absorbing or emitting nuclides, can cause variations in the local $^{236}U/^{238}U$ isotope ratio. The present result demonstrates that, once a material standard is established, different samples with different isotope ratios can be characterized and compared with high accuracy. Even though the inconsistency between our data and the previous measurements still has to be resolved, it has been demonstrated that calorimetric detectors can considerably improve the precision of such a material standard.

B. Sample from Bad Gastein

Due to the low uranium concentration, the amount of sample material for this sample was limited, and only one measurement of 20 min duration could be performed. The corresponding spectrum is displayed in Fig. 11. In the case of this sample, background is dominated by ^{234}U and yields approximately 30% of the total count rate. Therefore, at this level of sensitivity, background starts to play an important role, and a good energy resolution becomes more and more important for background separation.

The result for the isotope ratio, $^{236}U/^{238}U=(6.1\pm2.1)\times10^{-12}$ (see Table I), represents the smallest isotope ratio measured for $^{236}U/^{238}U$ up to date; the result was confirmed in recent measurements with the conventional setup and a larger amount of sample material.[20] As compared to measurements with a conventional setup (see Ref. 4 and Table I), sensitivity was enhanced by one order of magnitude by increasing the transmission from 31% to 65%. The error of this result is dominated by the statistical error. With a detection efficiency of 100% and a further improvement in the resolving power, it will be possible to reduce this error even if an increase in sample material is not easily achievable.

VI. DEVELOPMENT OF LARGER SOLID ANGLE ARRAYS—STATUS AND PERSPECTIVES

As discussed in Sec. VII, the current performance of calorimetric detectors in heavy ion physics is limited mainly by their active detector area of approximately 6 mm^2. Whereas for AMS applications such as the measurement of the $^{236}U/^{238}U$ ratio an active area of around 100 mm^2 is suitable, other applications may require active detector areas as large as 2000–3000 mm^2. On the other hand, the active area of a single calorimetric detector is limited by its heat capacity. The performance of larger single detectors is deteriorated by a worse signal-to-noise ratio. Therefore, the development of large solid angle arrays of calorimetric detectors for heavy ions is of high interest.

However, the development of such an array poses a special challenge. Figure 12 shows examples of transition curves obtained for different detector pixels, which were photolithographically produced on one single sapphire wafer. As the transition temperature T_C sensitively depends on the microstructure of the aluminum film and details of the deposition process, it can differ for different pixels by more than 0.1 K. Considering the fact that each transition has a transition width of $\delta T\leq10$ mK only, it is not possible to run an array of several detectors with one common temperature regulation circuit. On the contrary, each detector pixel has to be adjusted to its individual operating temperature and temperature-stabilized separately. To realize individual temperature stabilization, a heating resistor consisting of a gold wire of 25 μm width and a thickness of 120 nm was deposited on the detector. Due to the small heat capacity of the detector pixel, the heater resistance of around 25 Ω is sufficient to heat the pixel and to stabilize it at its operating temperature.

A schematic view of a first prototype array of 5 $\times$2 pixels is shown in Fig. 13. It consists of 5 columns with two pixels per column. Each column is independently replaceable. The detector pixels are glued to a ceramic carrier using Stycast epoxy. As the ceramic carrier is supposed to have a very low heat conductivity, the main link to the heat sink is realized via four gold wires of 25 μm in diameter, which also serve as electric connectors for signal readout. The inlay shows a close-up of a single pixel with the bonded gold wires and the additional heater on the left.

As an improvement of the cryogenic setup, a new pumped ^{4}He bath cryostat was developed, which has been especially adapted to the needs of heavy ion research.[21] Special care was taken to realize a high cooling power so that an

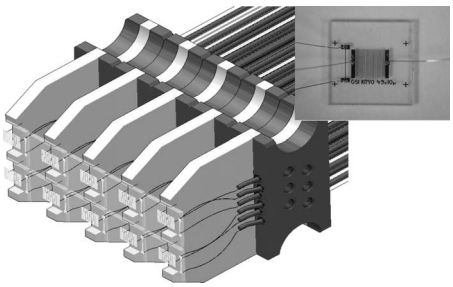

FIG. 13. Design of a prototype array consisting of 5×2 detector pixels. Each column of two pixels is mounted individually. The inlay shows one single pixel with the new design with the gold heater (Ref. 21).

active detector area of 30×80 mm^2 can be cooled to a base temperature of 1.2 K without using foils for thermal decoupling. Furthermore, the cryostat has to maintain a temperature of 1.2–1.5 K for many hours in stable operation. As the temperature stabilization has to be independent for more than 100 pixels, the thermal coupling of the individual pixels to the cold finger had to be chosen much smaller than the thermal coupling of the cold finger to the heat sink. To reduce thermal fluctuations due to cross-talk of the individual temperature regulations, the cold finger consists of a relatively large copper mass of 2 kg, strongly coupled to the helium bath. To minimize thermal irradiation from the surroundings, apertures with areas varying according to the active detector area can be mounted.

In a first step, an array of 3×2 detector pixels was produced and tested at the Gesellschaft für Schwerionenforschung (GSI) Darmstadt, Germany. Its response to heavy ion irradiation was investigated using ^{152}Sm ions at $E=547.2$ MeV and ^{64}Ni ions at $E=307.2$ MeV. To adapt the detectors for the relatively high ion energies, the transition widths of the detectors in this experiment were chosen around $\delta T\sim25$ mK. To adjust the count rate on the detector pixels, the ions were elastically scattered off a gold target under scattering angles between 3° and 10°. A detailed description of the experimental setup can be found in Ref. 22.

The results of the measurements are summarized in Table II. In average, a relative energy resolution of $\Delta E/E\approx8.0(3)\times10^{-3}$ was obtained. This result is comparable with the relative energy resolution of $\Delta E/E=6.93(5)\times10^{-3}$ achieved in the range of low ion energies (see paragraph 3).

TABLE II. Performance of the prototype array under irradiation with heavy ions. The notation a and b in the detector names refer to two pixels in the same column, i.e., on the same ceramic carrier. In average, a relative energy resolution of $\Delta E/E\approx8.0(3)\times10^{-3}$ was obtained.

	^{152}Sm, $E=547.2$ MeV	^{64}Ni, $E=307.2$ MeV
Pixel	$\Delta E/E[10^{-3}]$	$\Delta E/E[10^{-3}]$
D001-1[a]	7.0(4)	6.5(3)
D001-2	7.5(2)	9.6(3)
D002-1[b]	7.0(4)	6.6(3)
D002-2	7.8(2)	9.8(3)
D004-1	6.1(2)	7.7(3)
D004-2	9.9(4)	10.8(3)

[a]In the experiment with ^{64}Ni ions, this detector was shielded with an aperture of 0.5 mm in diameter.
[b]In the experiment with ^{64}Ni ions, this detector was shielded with an aperture of 1.0 mm in diameter.

To investigate a potential local dependence of the detector response function, in the experiment with ^{64}Ni ions two detectors were shielded by apertures to focus the ion interaction region in the detector center. The detector D001-1 was shielded with an aperture of 0.5 mm in diameter, the detector D001-2 with an aperture of 1.0 mm in diameter, respectively. Both detectors show an improved performance with a relative energy resolution of $\Delta E/E=6.6(3)\times10^{-3}$.

To exclude any influence of the scattering foils, the detectors D001-1 and D001-2 were irradiated with a strongly attenuated direct accelerator beam of ^{152}Sm ions. With the direct beam, again only a very small region of the detectors was illuminated. The results of this measurement are displayed in Fig. 14. The achieved energy resolution was considerably improved to $\Delta E/E=1.6(1)\times10^{-3}$ for D001-1 and $\Delta E/E=0.9(1)\times10^{-3}$ for D001-2, respectively. These values are already comparable with the intrinsic energy width of the UNILAC accelerator at GSI Darmstadt and represent the best performance achieved with these detectors up to now.

In conclusion, it can be stated that the principle of individual temperature stabilization has been demonstrated to operate successfully with up to 6 detector pixels. The energy resolution of individual pixels is not influenced by the temperature stabilization of surrounding pixels. As a next step, the number of pixels per column will be increased to achieve the required active area.

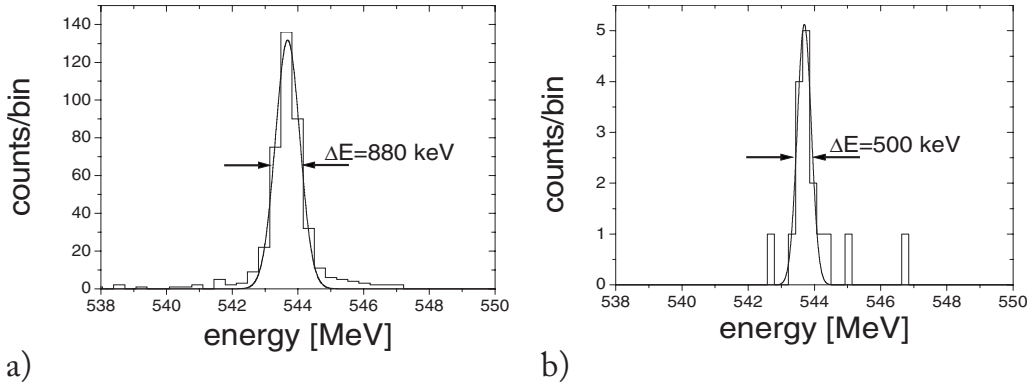

FIG. 14. Spectra obtained with direct-beam irradiation with ^{152}Sm ions of the detectors (a) D001-1 and (b) D001-2. The relative energy resolutions obtained were $\Delta E/E=1.6(1)\times10^{-3}$ for D001-1 and $\Delta E/E=0.9(1)\times10^{-3}$ for D001-2, respectively.

VII. CONCLUSION AND PERSPECTIVES

It has been demonstrated that calorimetric low temperature detectors achieve a very good energy resolution of $\Delta E/E=(4.6-6.9)\times 10^{-3}$ for heavy ions in the energy range of $E=5-60$ MeV. As compared to conventional ionization detectors, this corresponds to an improvement in energy resolution by one order of magnitude. The improvement is mainly due to the fact that with calorimetric detectors only a negligible fraction of the particle energy is lost in the detection process. This fact is proven by the perfectly linear energy response function of the detector and the absence of any pulse height defect. To further improve the energy resolution, several possibilities are currently under investigation. As ions in the energy range investigated have ranges in sapphire of several microns only, the absorber heat capacity can be considerably reduced by using thinner absorbers. In addition, other absorber materials such as diamond could provide advantage in terms of heat capacity and thermalization. To increase the active area of the detector, the development of a detector array is mandatory. As a first step, an array with 6 pixels and an area of about 100 mm^2 was tested successfully under heavy ion irradiation at relatively high ion energies of $E=300-600$ MeV. The achieved energy resolution of $\Delta E/E=(1-2)\times 10^{-3}$ is among the best achieved with this type of detectors. A potential local dependence of the detector response function is still under investigation.

A single calorimetric detector was applied in an AMS measurement to determine the isotope ratio $^{236}U/^{238}U$ in several samples with high precision. Due to the improved transmission, the sensitivity could be increased by one order of magnitude as compared to a conventional detection system. For the sample Bad Gastein, an isotope ratio of $^{236}U/^{238}U=(6.1\pm 2.1)\times 10^{-12}$ has been measured, representing the smallest isotope ratio for $^{236}U/^{238}U$ ever measured at the time. With a detector array of larger active area, transmission can be improved to almost 100%, so that the systematic error will be negligible. Further improvement in energy resolution will allow even better background suppression. Both factors will provide further enhancement in sensitivity.

Another potential application of calorimetric detectors in heavy ion physics is the direct mass identification of reaction products, especially so-called *superheavy elements*, via a combined energy/TOF measurement. Results of first test experiments are encouraging. However, to exploit this application in greater detail, a detector array with an active detector area of 30×80 mm^2 is mandatory.[7]

[1] W. Kutschera, Int. J. Mass Spectrom. **242**, 145 (2005).
[2] S. Richter, A. Alonso, W. De Bolle, R. Wellum, and P. D. P. Taylor, Int. J. Mass Spectrom. **193**, 9 (1999).
[3] C. Vockenhuber, I. Ahmad, R. Golser, W. Kutschera, V. Liechtenstein, A. Priller, P. Steier, and S. Winkler, Int. J. Mass Spectrom. **223–224**, 713 (2003).
[4] P. Steier, R. Golser, W. Kutschera, A. Priller, A. Valenta, C. Vockenhuber, and V. Liechtenstein, Nucl. Instrum. Methods Phys. Res. B **188**, 283 (2002).
[5] H. H. Andersen, Nucl. Instrum. Methods Phys. Res. B **15**, 722 (1986).
[6] P. Egelhof, Adv. Solid State Phys. **39**, 61 (1999) (and references therein).
[7] P. Egelhof and S. Kraft-Bermuth, in *Cryogenic Particle Detection*, Topics in Applied Physics Vol. 99, edited by Chr. Enss (Springer-Verlag, Berlin, 2005), pp. 469–498.
[8] *Cryogenic Particle Detection*, Topics in Applied Physics Vol. 99, edited by Chr. Enss (Springer-Verlag, Berlin, 2005).
[9] D. McCammon, in *Cryogenic Particle Detection*, Topics in Applied Physics Vol. 99, edited by Chr. Enss (Springer-Verlag, Berlin, 2005), pp. 1–34.
[10] A. v. Kienlin, F. Azgui, W. Böhmer, K. Djotni, P. Egelhof, W. Henning, G. Kraus, J. Meier, and K. W. Shepard, Nucl. Instrum. Methods Phys. Res. A **368**, 815 (1996).
[11] H. J. Meier, L. Chulkov, P. Egelhof, C. Fischer, W. Henning, A. v. Kienlin, G. Kirchner, G. Kraus, and A. Weinbach, Nucl. Instrum. Methods Phys. Res. A **370**, 259 (1996).
[12] H. J. Meier, P. Egelhof, W. Henning, A. v. Kienlin, G. Kraus, and A. Weinbach, Nucl. Phys. A **626**, 451 (1997).
[13] P. Steier, S. Puchegger, R. Golser, W. Kutschera, A. Priller, W. Rom, A. Wallner, and E. Wild, Nucl. Instrum. Methods Phys. Res. B **161–163**, 250 (2000).
[14] S. Kraft-Bermuth, V. Andrianov, A. Bleile, P. Egelhof, R. Golser, A. Kiseleva, O. Kiselev, W. Kutschera, J. P. Meier, A. Priller, A. Shrivastava, P. Steier, and C. Vockenhuber, Nucl. Instrum. Methods Phys. Res. B **520**, 63 (2004).
[15] S. Kraft, A. Bleile, P. Egelhof, R. Golser, O. Kisselev, W. Kutschera, V. Liechtenstein, H. J. Meier, A. Priller, A. Shrivastava, P. Steier, C. Vockenhuber, and M. Weber, AIP Conf. Proc. **605**, 405 (2002).
[16] V. A. Andrianov, A. Bleile, P. Egelhof, S. Kraft, A. Kiseleva, O. Kiselev, H. J. Meier, and J. P. Meier, Nucl. Instrum. Methods Phys. Res. A **520**, 84 (2004).
[17] J. Lindhard, V. Nielsen, M. Scharff, and P. V. Thomsen, Mat. Fys. Medd. K. Dan. Vidensk. Selsk. **33**, 3 (1963).
[18] S. Kraft-Bermuth, Ph.D. thesis, Johannes Gutenberg Universität Mainz, 2004.
[19] K. M. Wilcken, T. T. Barrows, L. K. Fifield, S. G. Tims, and P. Steier, Nucl. Instrum. Methods Phys. Res. B **259**, 727 (2007).
[20] P. Steier, M. Bichler, L. K. Fifield, R. Golser, W. Kutschera, A. Priller, F. Quinto, S. Richter, M. Srncik, P. Terrasi, L. Wacker, A. Wallner, G. Wallner, K. M. Wilcken, and E. M. Wild, Nucl. Instrum. Methods Phys. Res. B **266**, 2246 (2008).
[21] S. Kraft-Bermuth, A. Bleile, P. Egelhof, S. Ilieva, A. Kiseleva, O. Kiselev, and J. P. Meier, Nucl. Instrum. Methods Phys. Res. B **559**, 519 (2006).
[22] A. Echler, Diploma thesis, Johannes Gutenberg Universität Mainz, 2007.

AUTHOR QUERIES — 024909RSI

#1 Au: please check changes in the affiliation.
#2 Au: Please verify edits in the sentence “One sample investigated…” to make sure your meaning was preserved.
#3 Au: Please verify edits in the sentence “As the uranium…” to make sure your meaning was preserved.
#4 Au: please check renumbering of Refs. 20–22.
#5 Au: please check citation of Sec. VII.
#6 Au: please verify insertion of authors in Ref. 2.
#7 Au: please verify edits in Ref. 7.
#8 Au: please verify edits in Ref. 8.
#9 Au: please note change to page number in Ref. 12 to match our database.
#10 Au: please verify insertion of authors in Ref. 13.
#11 Au: please verify accuracy and insertion of authors in Ref. 14.
#12 Au: please verify insertion of authors in Ref. 15.
#13 Au: please check journal title in Ref. 17.
#14 Au: please verify insertion of authors in Ref. 19.
#15 Au: please verify insertion of authors in Ref. 20.
#16 Au: please verify insertion of authors in Ref. 21.
#17 Au: please verify edits in Ref. 22.